Supplemental Material: Nanostar Self-Assemblies of Spherical Nanoparticles inside Lipid Vesicles

Yu Zhu,[a,b] Abash Sharma,[a,c] Eric J. Spangler,[a] and Mohamed Laradji[a]

[a] *Department of Physics and Materials Science, The University of Memphis, Memphis, TN 38152, USA*

[b] *Borch Department of Medicinal Chemistry and Molecular Pharmacology, Purdue University, Lafayette, IN 47907, USA*

[c] *Department of Bioinformatics, University of Texas Southwestern Medical Center, Dallas, TX 75390, USA*

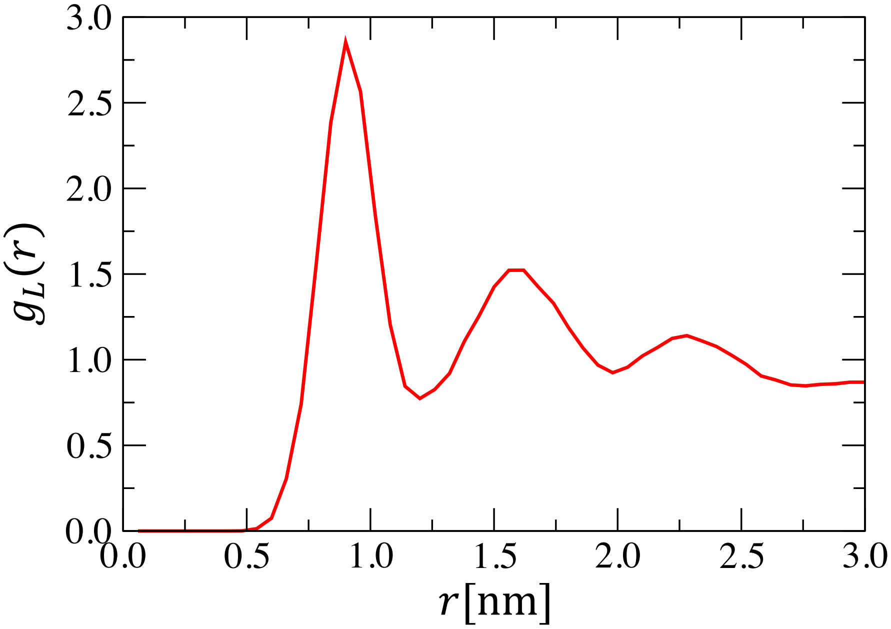

FIG. S1. Radial distribution function of lipid beads based on the model with the parameters given by Table 1 in the article.

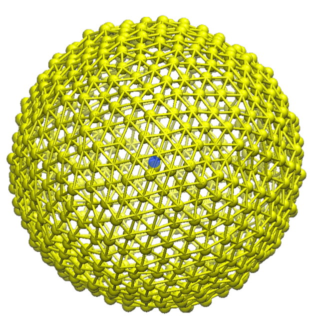

FIG. S2. A snapshot of an equilibrated 20-nm spherical NP. The n beads are yellow, and the blue bead corresponds to the c bead at the center of the NP. The n beads are connected by yellow links.

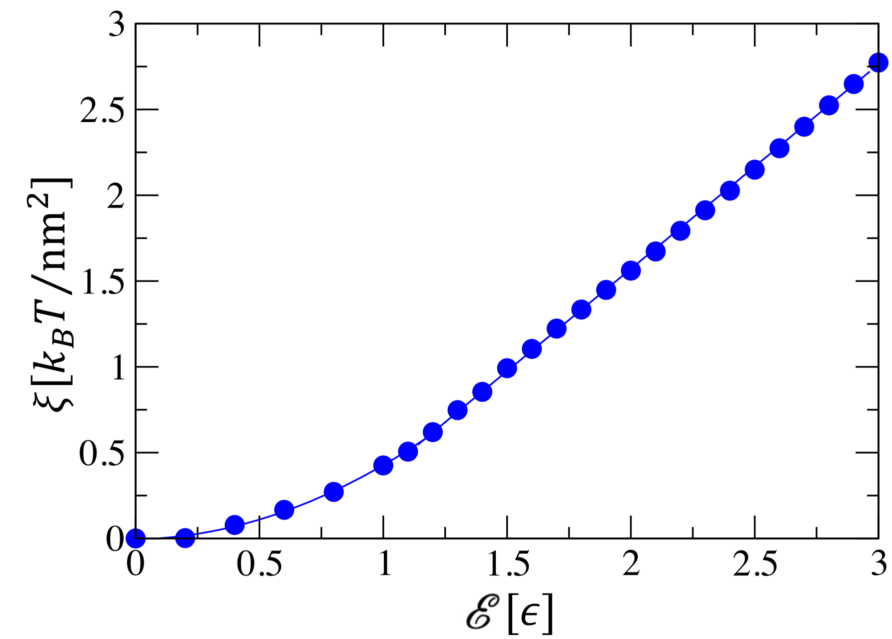

FIG. S3. The adhesion energy density ξ vs the interaction strength $\mathcal{E} = -U_{\min}^{nh}$ between an h-bead and an n-bead. ξ is determined from simulations of a 20-nm spherical NP adhering to a planar tensionless membrane, with periodic boundary conditions along the lateral directions, at different values of $\mathcal{E} = U_{\min}^{nh}$.

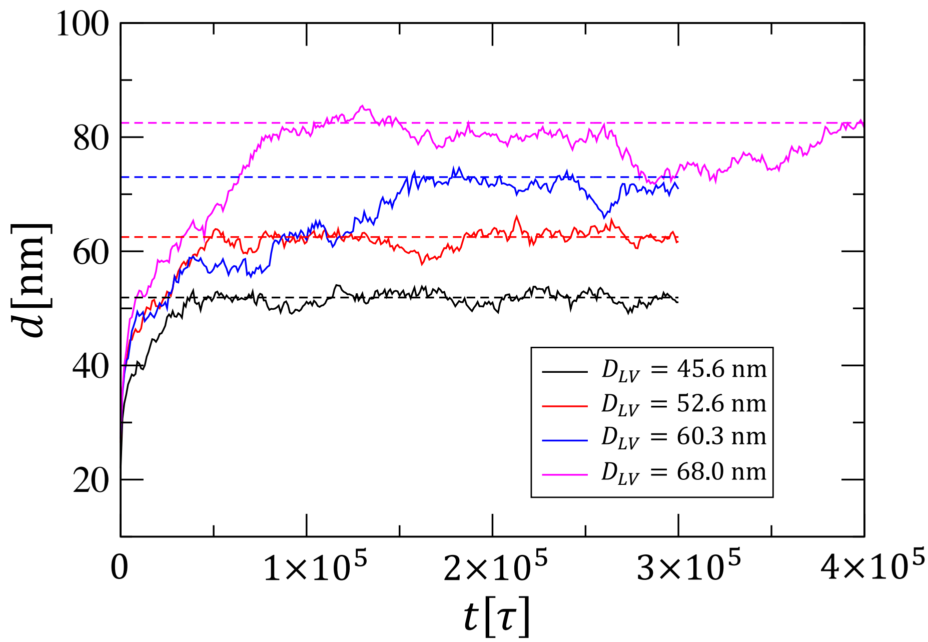

FIG. S4. Distance between two 20-nm NPs adhering to the inner side of a vesicle with diameter D_{LV} at $\xi = 0.62 k_BT/\mathrm{nm}^2$. The values of d of the horizontal dashed lines correspond to the minimum of the free energy in Fig. 1 (A).

DISCUSSION OF POSITIONS OF PEAKS OF THE RDFS

In the case of $n = 4$, we found that $r_2/r_1 = 1.39$, which is slightly smaller than the ideal ratio of $\sqrt{2}$ in the case of a square. In the case of $n = 5$, we found that $r_2/r_1 = 1.61$, which is very close to the value of the regular pentagon,

$(1+\sqrt{5})/2 \approx 1.62$. For $n=6$, $r_2/r_1 = 1.72$ and $r_3/r_1 = 1.99$. These values are very close to the corresponding of a regular hexagon, which are respectively $\sqrt{3} \approx 1.73$ and 2. Similarly, in the case of $n=7$, $r_2/r_1 = 1.80$ and $r_3/r_1 = 2.23$. These are also very close to the corresponding ratios of a regular heptagon, which are respectively $2\cos(\pi/7) \approx 1.80$ and $4\cos^2(\pi/7) - 1 \approx 2.25$. Fig. 9 (B) shows that in the case of $n=8$, the third and fourth peaks overlap. The positions of these two peaks are resolved by fitting the RDF in this region with the sum of two Gaussians. In this case, $r_2/r_1 = 1.84$, $r_3/r_1 = 2.42$, and $r_4/r_1 = 2.67$. These are also very close to their counterparts of a regular octagon, corresponding respectively to $\sqrt{2+\sqrt{2}} \approx 1.85$, $1+\sqrt{2} \approx 2.41$, and $\sqrt{4+2\sqrt{2}} \approx 2.61$. In the case of $n=9$, $r_2/r_1 = 1.87$, $r_3/r_1 = 2.51$, and $r_4/r_1 = 2.85$. These are also very close to their ideal values in the case of a regular nonagon, corresponding respectively to $2\cos(\pi/9) \approx 1.88$, $4\cos^2(\pi/9) - 1 \approx 2.53$, and $4\cos(\pi/9)\cos(2\pi/9) \approx 2.88$. Finally, in Fig. 9 (B), the RDF for the case of $n=10$ seems to exhibit only four peaks, while an ideal decagon has five peaks. However, the breadth of the 4th peak hints at the fact that it is the overlap of two close peaks. A fit of the last two peaks can be fitted with the sum of three Guassians (see inset of Fig. 9 (B)). The obtained ratios for $n=10$ are then $r_2/r_1 = 1.88$, $r_3/r_1 = 2.58$, $r_4/r_1 = 3.04$, and $r_5/r_1 = 3.11$. These values are again close to their regular decagon counterparts, which are, respectively, $\sqrt{(5+\sqrt{5})/2} \approx 1.90$, $\sqrt{(7+3\sqrt{5})/2} \approx 2.62$, $\sqrt{5+2\sqrt{5}} \approx 3.08$, and $1+\sqrt{5} \approx 3.24$. These results imply that the NPs' nanoassemblies inside vesicles have indeed ordered polygonal star-like geometries.

TABLE I. Ratios r_i/r_1 for different values of n. r_i is the position of the ith RDF peak. In each cell, the top value corresponds to the position of r_i/r_1 in the RDF, and the bottom value is its counterpart for a regular polyhedron with n vertices.

n	r_2/r_1	r_3/r_1	r_4/r_1	r_5/r_1
4	1.39			
	$2^{1/2} \approx 1.41$			
5	1.61			
	$(1+5^{1/2})/2 \approx 1.62$			
6	1.72	1.99		
	$3^{1/2} \approx 1.73$	2		
7	1.80	2.23		
	$2\cos(\pi/7) \approx 1.80$	$4\cos^2(\pi/7) - 1 \approx 2.25$		
8	1.84	2.42	2.67	
	$(2+2^{1/2})^{1/2} \approx 1.85$	$1+2^{1/2} \approx 2.41$	$(4+2^{3/2})^{1/2} \approx 2.61$	
9	1.87	2.51	2.85	
	$2\cos(\pi/9) \approx 1.88$	$4\cos^2(\pi/9) - 1 \approx 2.53$	$4\cos(\pi/9)\cos(2\pi/9) \approx 2.88$	
10	1.88	2.58	3.04	3.11
	$[(5+5^{1/2})/2]^{1/2} \approx 1.90$	$[(7+3\times 5^{1/2})/2]^{1/2} \approx 2.62$	$[5+2\times 5^{1/2}]^{1/2} \approx 3.08$	$1+5^{1/2} \approx 3.24$

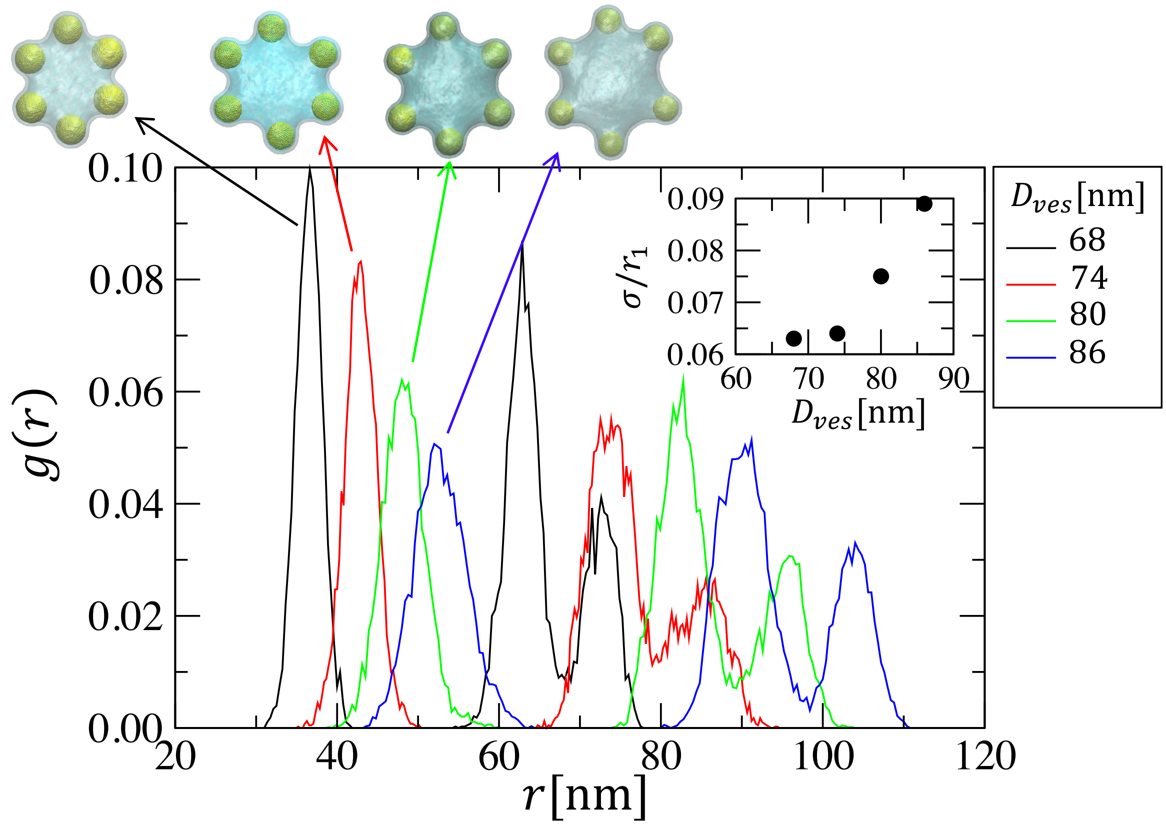

FIG. S5. Radial distribution function, $g(r)$, for four different values of D_{LV}, in the case of $n = 6$ and $\xi = 1.4 k_B T/\mathrm{nm}^2$. Also shown are equilibrium snapshots corresponding to the four values of D_{LV}. (Inset) Ratio σ/r_1 versus D_{LV}, where σ is the width of the first peak of the RDF and r_1 is the position of the first peak.

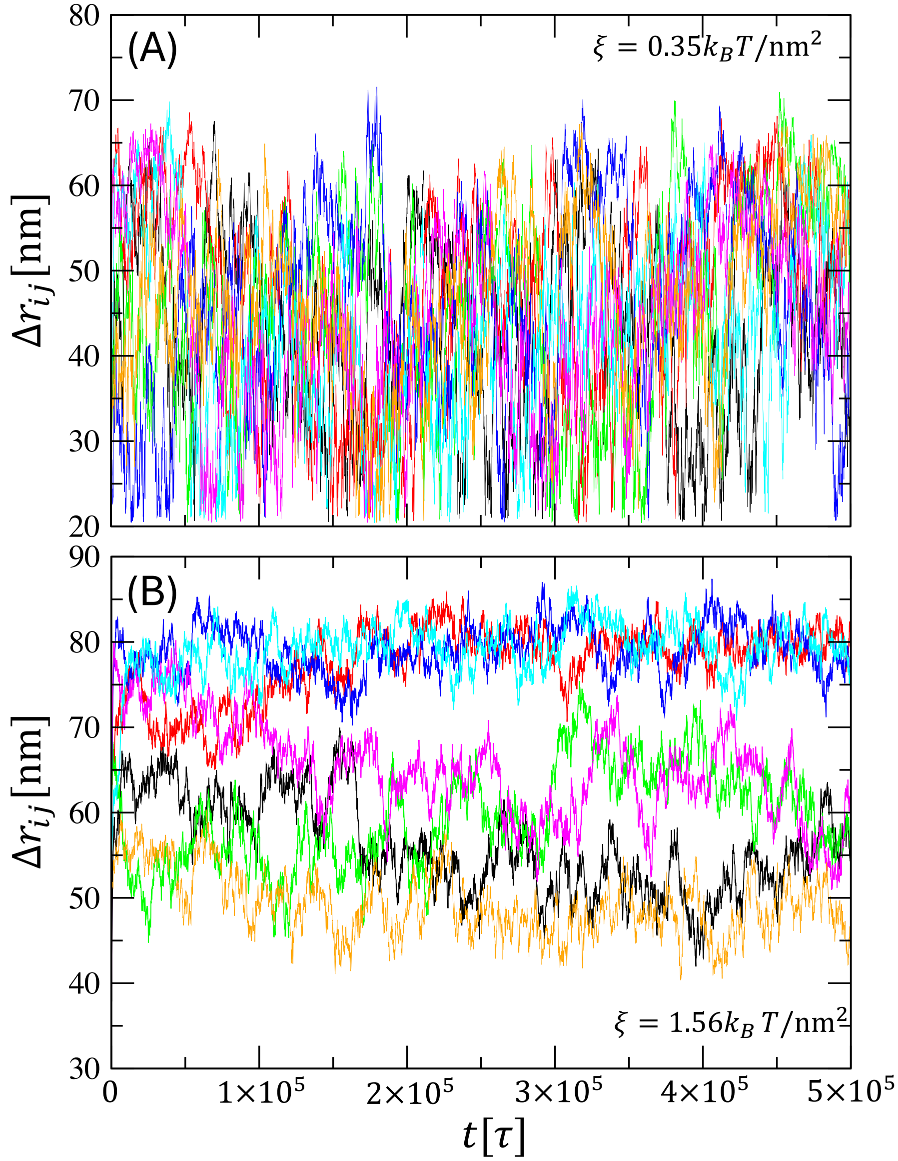

FIG. S6. Distance between NPs in the vesicle as a function of time of 7 NPs' pairs in the case of $n = 6$ and $\rho = 2.31$ at $\xi = 0.35 k_B T/\mathrm{nm}^2$ (A) and $\xi = 1.56 k_B T/\mathrm{nm}^2$ (B). Note that at low adhesion strength ($\xi = 0.35 k_B T/\mathrm{nm}^2$), the distances exhibit a large amount of fluctuations, resulting from their high diffusivity. In contrast, the amount of fluctuations in the distances is much weaker at high ξ. This implies that NPs at high ξ are localized inside the vesicle.

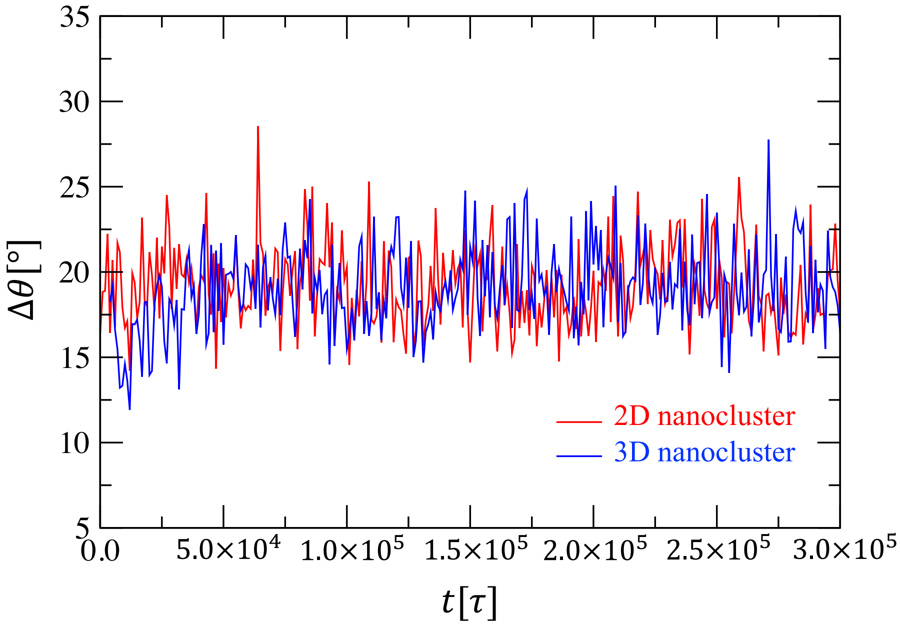

FIG. S7. Time evolution of $\Delta\theta = \theta_{max} - \theta_{min}$ at $\xi = 2.03k_BT/\mathrm{nm}^2$, $n = 6$ and $\rho = 2.31$. The red curve corresponds to the case where the NPs form a two-dimensional cluster (as obtained from an upward annealing starting from a low value of ξ). The blue curve corresponds to the case where the NPs form a three-dimensional cluster (as obtained from a direct simulation of 6 NPs inside the vesicle at the same value of ξ).